Available online www.jsaer.com

***Journal of Scientific and Engineering Research*, 2020, 7(9):16-24**

Research Article

ISSN: 2394-2630
CODEN(USA): JSERBR

Determination of Tectonic Structure in Marmara Region Using Markov Random Fields Method

Ali Muhittin Albora

Istanbul University-Cerrahpaşa, Engineering Faculty, Geophysical Department, 34850, Büyükçekmece-Istanbul, Turkey
Email: muhittin@istanbul.edu.tr

Abstract In this study, it was aimed to determine the discontinuity limits by using Markov Random Fields (MRF) method in gravity anomaly maps. As it is known, one of the most important issues in potentially sourced areas is to reveal the building boundaries of geological structures. For this purpose, the Markov Random Field (MRF) method was applied to the gravity anomaly map of the Marmara region and possible fault lines were determined. The most important feature of the MRF method is that it uses the stochastic features of the neighborhood and two-dimensional image and does not require pre-training. The Marmara region gravity anomaly map was used as a field study. The tectonic structure of the Marmara region was revealed from the map we obtained using the MRF method. While revealing the tectonic lines belonging to the Marmara region, comparisons were made using the seismic, topographic and bathymetric data previously made in the region.

Keywords Markov Random Field (MRF), Marmara Region, Boundary dedection

Introduction

Filter techniques are one of the most important issues in the interpretation of potentially sourced anomaly maps. It is one of the most important problems in geophysical engineering to reveal geological structures by separating regional and residual anomalies. The image processing techniques currently used in Electronics Engineering make important contributions to the solution of these problems in geophysical engineering. A good filter of potentially sourced anomaly maps makes it significantly easier for us to find the parameters of geological structures in a realistic way. In order to show that the MRF method works successfully, studies on synthetic data were performed first, and it was found that the MRF method gave more successful results than conventional filters used in Geophysical Engineering [1]. The most important feature of the MRF method can be summarized as considering neighborly relations, benefiting from the stochastic structure of the two-dimensional image, not requiring pre-education and very little data loss. The first application of the MRF approach to two-dimensional images was made by [2-4]. They performed the solution of potential geophysical problems of MRF method [5-10]. MRF approach, which is frequently used in filtering processes in electronic engineering, has been applied to the Gravity anomaly map obtained by the Mineral Research Exploration Institute (MTA) in the Marmara region. It is known that there are many active faults that can produce earthquakes in the Marmara region. For this reason, knowing the tectonic structure of the Marmara region in detail is very important in terms of knowing the fault lines that will produce earthquakes. For this purpose, this study was carried out to reveal the building boundaries and obtain a tectonic map by applying MRF method to the gravity anomaly map of the Marmara region.

Method

Markov Random Fields Method

In this study, gravity anomaly map was taken as *N1xN2* dimensional y={y_{ij}} image. It is assumed that this image consists of the interaction of different structures underground. With MRF application, residual structures were revealed and x={x_{ij}}. The random variable X is called $Q=\{q_1,q_2,q_3,...q_M\}$ and M takes one of the quanta value.

The transition from the Y anomaly map to the X residual map conforms to the Bayesian rule, and the probability of the transition is $P(X=x|Y=y)$,

$$P(X=x|Y=y)=\frac{P(Y=y|X=x)P(X=x)}{P(Y=y)} \quad (1)$$

If this formula is maximum and its logarithmic expression,

$$\ln P(X=x|Y=y)=\ln P(X=x)+\ln P(X=x|Y=y), \quad (2)$$

It shaped. Equality 3 and 4 are obtained by doing some operations on Equation 2.

$$\ln P(X=x)=-\ln Z-\sum_{c\in C}V_c(x), \quad (3)$$

$$\ln P(Y=y|X=x)=-\frac{N_1N_2}{2}\ln(2\pi\sigma^2)-\sum_{m=1}^{M}\sum_{(i,j)\in S_m}\frac{1}{2\sigma^2}(s_{ij}-q_m')^2 \quad (4)$$

It shaped.

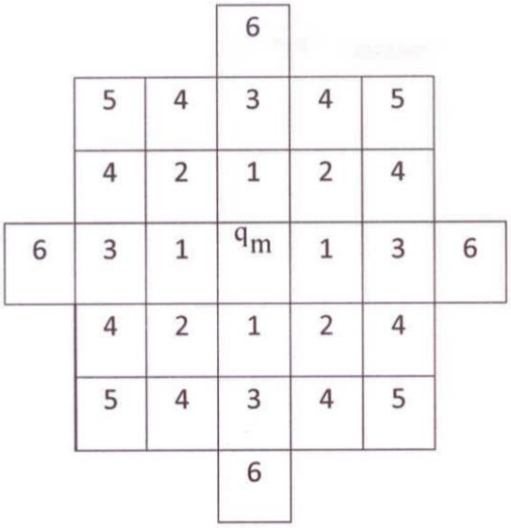

Figure 1: System showing the neighborhood relationship in a regular manner

Here sm={(i,j) $\in L: X_{ij}=m$ }. Z is a constant, qm 'is the temporal quanta level. Figure 1 shows the neighborhood relationships of qm.

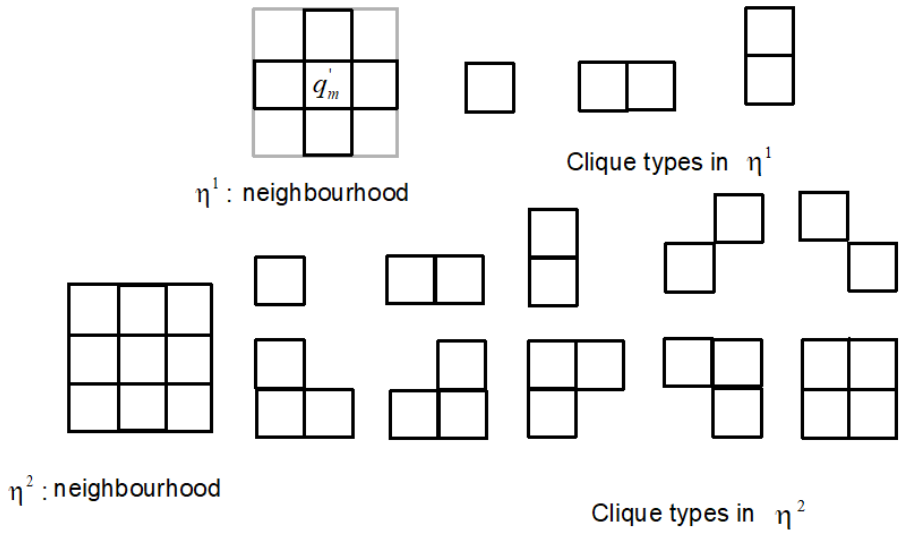

Figure 2: Representation of η^1, η^2 and other components in the neighborhood system

$V_c(x)$ is the potential due to clicks [3]. $q_m^{'}$ can be written in terms of neighborhood relationship as follows. Figure 2 shows the nü 1 and nü 2 neighborhood components in the neighborhood system.

$$t^{'} = [u1, u2, u3, u4, v1, v2, v3, v4]^{T} \quad (5)$$

Here $t^{'}$ gives neighborhood. If intermediate operations are omitted, the right side of equation-3 can be written as follows (Figure-3).

$$V(q_m^{'}, t', \theta) \equiv \sum_{c: q_m^{'} \in C} V_C(x) \quad (6)$$

$$\theta = [\alpha_1, \alpha_2, .., \alpha_M, \beta_1, \beta_2, \beta_3, \beta_4, \gamma_1, \gamma_2, \gamma_3, \gamma_4, \xi_1]^T, \quad (7)$$

where θ is the parameter vector and is defined below.

α, β, γ and ξ indicate neighborhood levels. Here, if Correlation-6 is reorganized,

$$V(q_m^{'}, t', \theta) \equiv \phi^T(q_m^{'}, t')\theta. \quad (8)$$

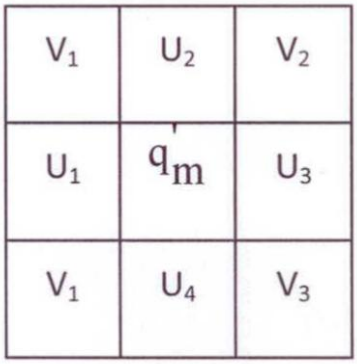

Figure 3: $q_m^{'}$ Designation terms of neighborhood relationships.

From here,

$$\phi(q_m^{'}, t') = [J_1(q_m^{'}), J_2(q_m^{'}), ..., J_M(q_m^{'}), (I(q_m^{'}, u_1) + I(q_m^{'}, u_3)), (I(q_m^{'}, u_2) + I(q_m^{'}, u_4)), (I(q_m^{'}, v_2) + I(q_m^{'}, v_4)), (I(q_m^{'}, v_1) + I(q_m^{'}, v_3)), (I(q_m^{'}, u_2, v_2) + I(q_m^{'}, u_4, u_3) + I(q_m^{'}, u_1 v_4)),$$

$$((I(q_m^{'},u_4,v_3)+I(q_m^{'},u_2,u_3)+I(q_m^{'},u_1,v_1)),(I(q_m^{'},u_2,v_1)+I(q_m^{'},u_1,u_4)$$
$$+I(q_m^{'},u_3,v_3)),(I(q_m^{'},u_1,u_2)+I(q_m^{'},u_4,v_4)+I(q_m^{'},u_3,v_2)),(I(q_m^{'},u_1,u_2)$$
$$+I(q_m^{'},u_1,v_1,u_2)+I(q_m^{'},u_2,v_2,u_3)+I(q_m^{'},u_3,v_3,u_4)+I(q_m^{'},u_4v_4,u_1))]^T \qquad (9)$$

writeable. Here *I* and *J* are indicator functions. Thus, MRF was obtained [see for details; 11].

Application of MRF method to Marmara Region Gravity data

Gravity anomaly study conducted in Marmara Region by General Directorate of Mineral Research and Exploration (M.T.A) and given in Figure-4 is used in this article. When the gravity anomaly map is examined, anomalies starting from the Istanbul Strait in front of the Bosphorus along the north shore of the Marmara Sea show a relatively low value to the west. It is known that these values mostly correspond to the depressions in the Sea of Marmara in bathymetry. Relatively high anomaly values are seen from Kapidag Peninsula to the north of Marmara Island, which indicates the presence of masses with high density. It is observed that the bathymetry is less inclined along the southern shelf of the Marmara Sea. On the other hand, it is understood from the frequency of the contours that the change of gravity values is greater in the Bouguer gravity anomaly map (Figure- 4).

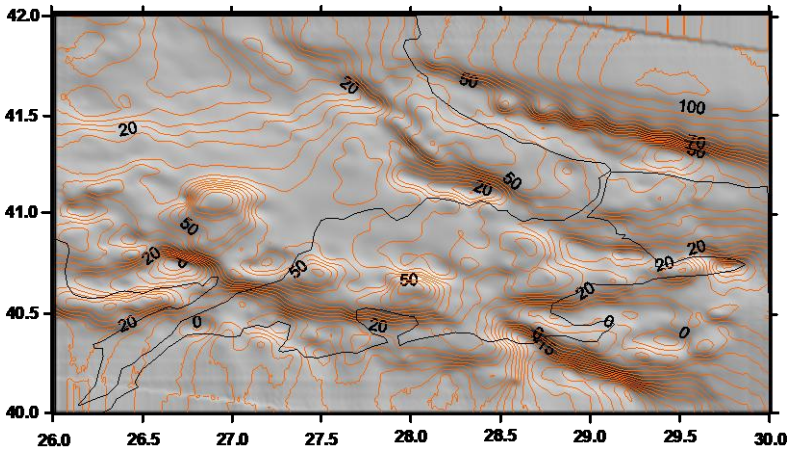

Figure 4: The relief and contour values of the Bouguer anomaly map of the Marmara region

It is possible to link this situation to the normal faults that are observed along the southern shelf of the Marmara Sea. There is a decrease in Gravity anomaly values in Thrace region. We can say that this stems from the Thracian cupping. Bouguer gravity values range from 2 to 50 mgal in Thrace Basin. Thick and young sediments with low densities create low gravity anomalies in the center of the Thrace basin. High gravity anomalies are evident in the north along with the Istranca Massif and in the south due to outcrops of Paleozoic basement rocks. These units contain igneous, metamorphic and ophiolitic rocks in some places [12]. MRF method was applied to the gravity anomaly map obtained in the Marmara region and the MRF output obtained is shown in Figure 5. When the map obtained from MRF printouts is examined, it is seen that the Thrace Eskişehir Fault Zone (TEFZ) comes from the north of the Bosphorus and extends towards the Kırklareli region. Again, it is observed that the North Anatolian Fault Zone (NAF) started by Eastern Anatolia, divided into branches in the Marmara Sea, passed through Saros Gulf under the name Ganos Fault and continued towards the Aegean Sea. In the south of the Marmara region, the Gönen Manyas Fault and Bandırma Fault and the southern branch of the NAF are clearly observed (Figure 5).

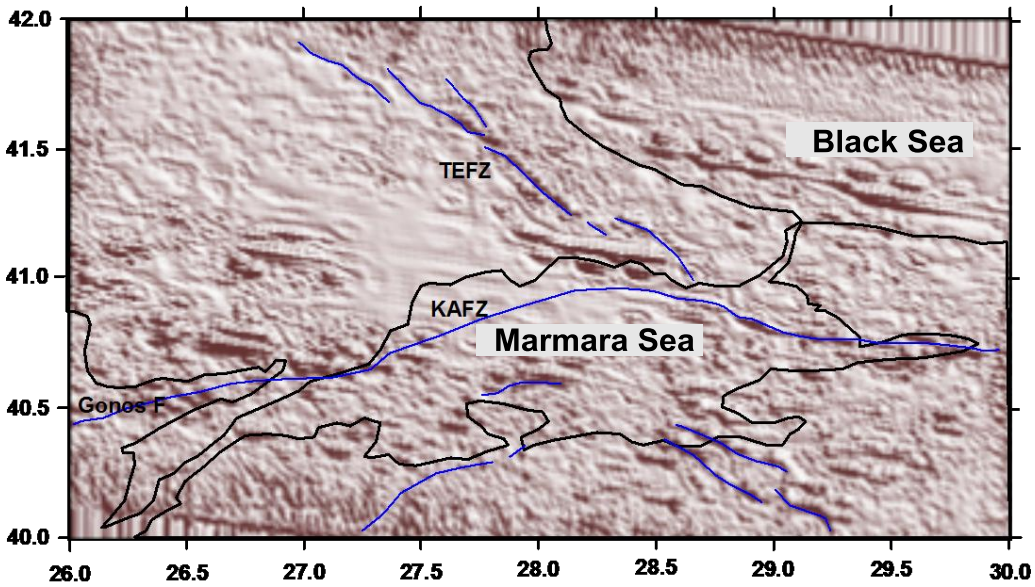

Figure 5: Markov Random Filter output of the bouguer anomaly map of the Marmara region

Geology of Marmara Region

It is an important geological event with the presence of the Thrace Tertiary Basin in the region (Figure 6). Thousands of meters of sedimentary and volcanic material have accumulated in this precipitation basin during the Cenozoic year. The Thrace Basin is surrounded by Istıranca mountains in the north and northeast, Rodop Massif in the west and Biga, Kapıdağı and Marmara Islands and Samanlıdağ massifs in the south. It is defined as a large and deep sedimentation bowl partially enclosed in the Marmara Sea, which is the continuation of the Thrace basin, which collapsed with the south-northwest fault line. This area is miocene aged rocks and alluvial grounds are observed in places where Ayancı stream, Çırpıcı stream, Yeşilköy, Büyük and Küçükçekmece lakes are formed in the north-south direction. The Armutlu peninsula to the south of the Marmara region consists of metamorphic rocks, and these metamorphic rocks formed the Çınarcık pit. The Kocaeli platform, which is bounded by the northern fault of the Çınarcık pit and the northern fault lines of Izmit, is located. This platform is observed until Istanbul and it is hard rocks made up of palesoic aged rocks [13].

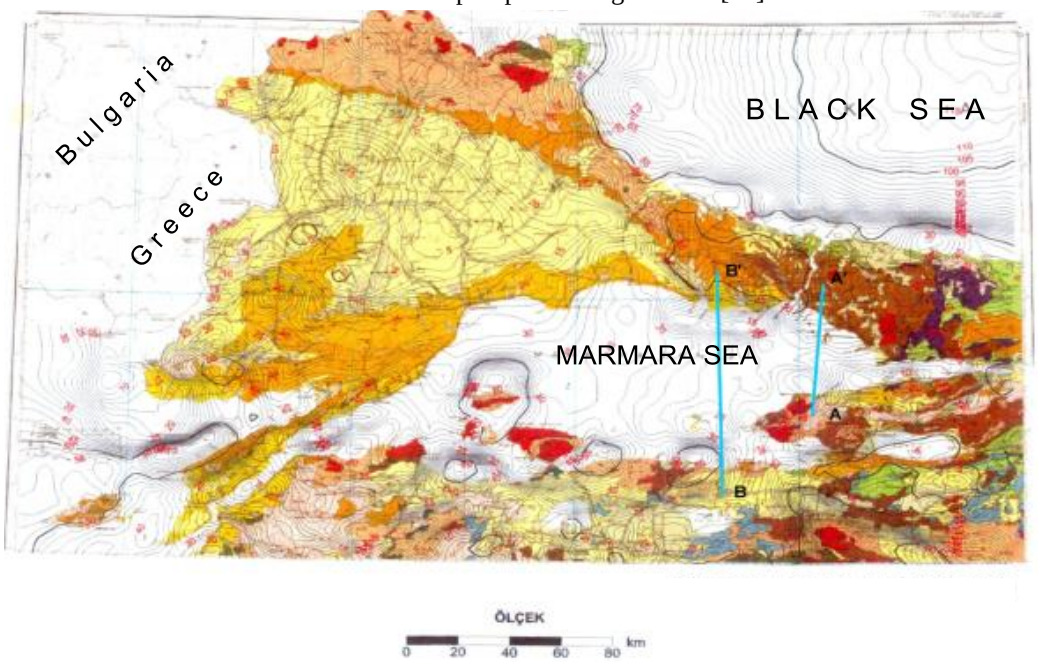

Figure 6: Bouguer anomaly Map and geology of Marmara and Thrace region (Taken from MTA)

Results and Discussion

Our aim in this study is to determine the structural boundaries of potential area data, to make a regional-residual separation of these data and to reveal the geological structures that create discontinuity by applying MRF method in the Gravity anomaly map of the Marmara region. For this purpose, it is aimed to illuminate the complex tectonism of the Marmara region by using MRF method. The most important feature of the MRF method over classical methods is that the dimensions of our input data are the same as our output data. In other words, there is no data loss on a map with MRF method. This provides a great advantage for us in our filter work. KAF entered the Marmara Sea with major earthquakes and changed the tectonic structure and geography of the region. After this incident, many large and small faults were formed both on land and in the sea. Many scientists defended the thesis that the waters of the Mediterranean entered the Saros Gulf and formed the Marmara Sea, which was previously a lake. For this reason, many authors examine the Aegean sea as part of the Mediterranean. However, the geological and tectonic structure of the Aegean Sea is quite different and complex than the Mediterranean.

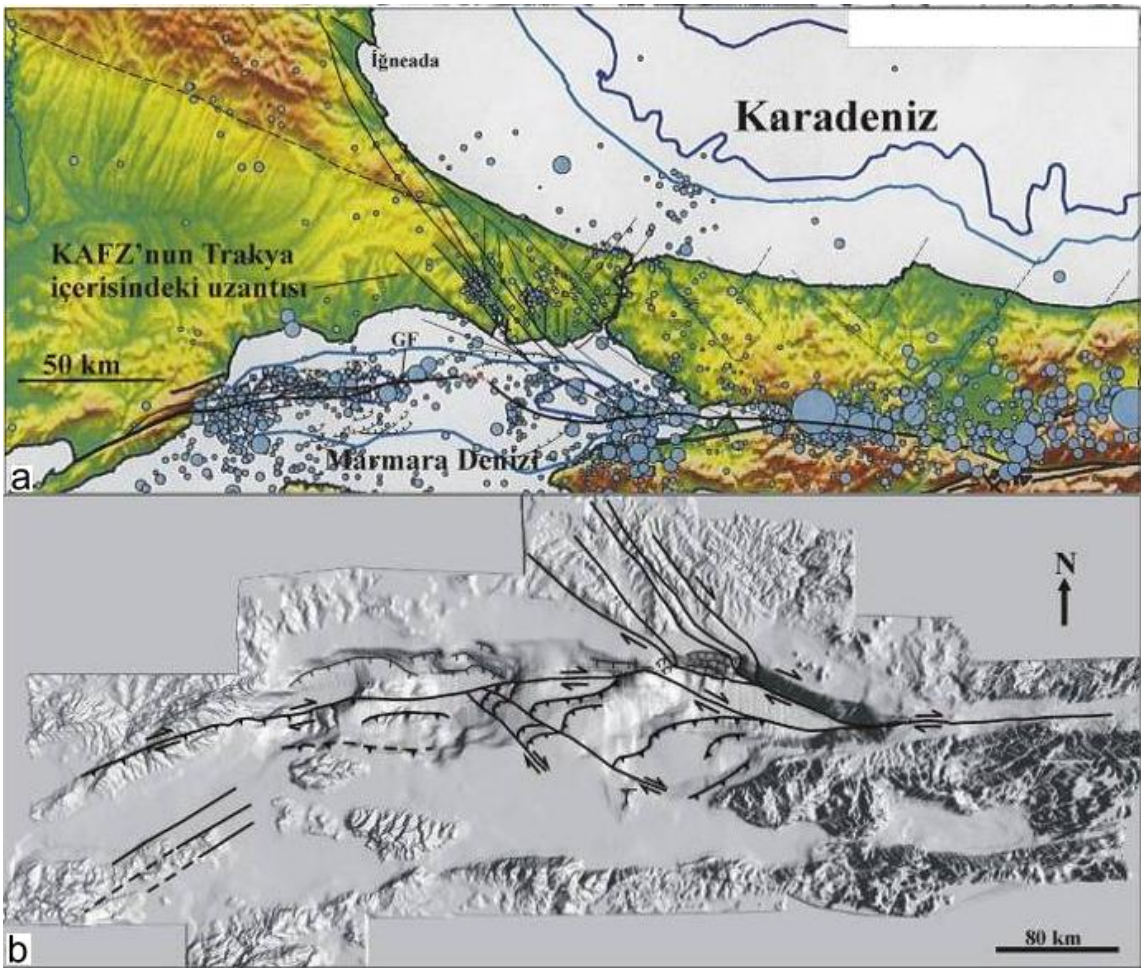

Figure 7: Marmara Sea with the help of detailed bathymetric data a) seismicity data [14], () active fault model [15]

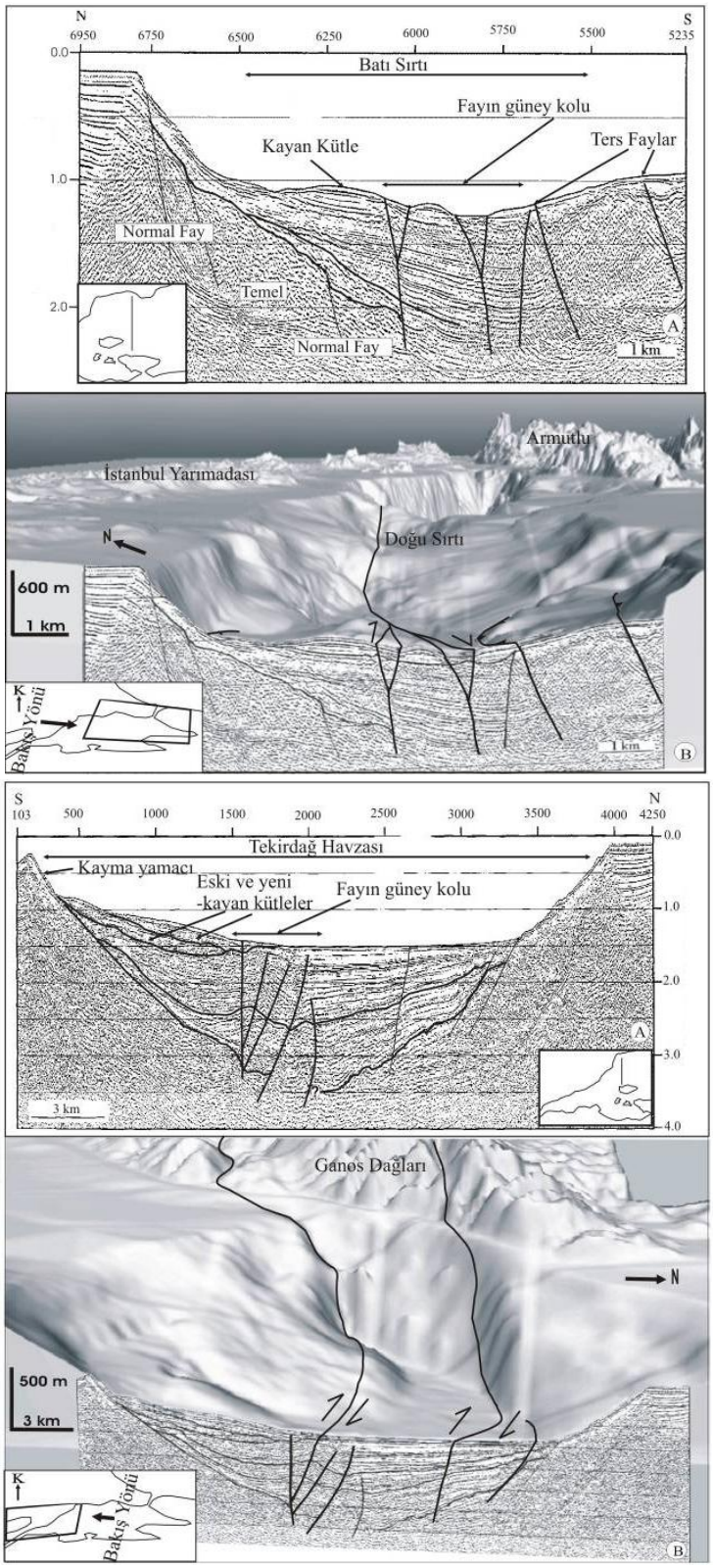

Figure 8: 3D model produced for Tekirdağ Basin and West Ridge as a result of using seismic and bathymetric data together and fault in this area [13]

MRF method was applied to the gravity anomaly map of the Marmara region and a light was attempted to shed light on the tectonic structure of the region. The map obtained as a result of MRF (13) was compared with the maps obtained by the bathymetric studies carried out in the Sea of Marmara in [14] (Figure 7). As a result of this

comparison, it was seen that very good results were obtained with the data obtained from the MRF output. As a result of the study, it was determined that there is a linearity that extends from the Ganos Mountain System to the Büyükçekmece offsets and cuts deeply between the deep basins and the ridges between them, and that significantly overlaps with the earthquake distributions in the Marmara Sea [13]. The results obtained after applying the MRF method to the Gravity measurements made in the region were also determined in this region. In Gökaşan et al. [14-15] have identified that the limiting faults have inactive or low activity today and this fault is the youngest fracture of the NAFZ developed in the Sea of Marmara, and the active tectonism of the Sea of Marmara is largely controlled by this fault (Figure 13). These results show that, as stated in [16], the activity of the northern branch of KAFZ and the formation of Marmara basins are different tectonic processes, or that KAFZ forms different steps within the evolution of northwest Anatolia. When MRF method is applied to Marmara region gravity anomaly maps, it is seen that the fault lines are clearly visible. As can be seen from the different studies on the Gravity and Magnetic maps of the Marmara region, [17-19] MRF method also shows successful results in determining the structure discontinuities.

Acknowledgement

Terrain data we have received the Mineral Research and Exploration Institute (MTA), Turkey Petroleum Corporation (TPAO), Navigation, Hydrography and Oceanography Directorate (shod) Thank you to the employees.

References

[1]. Albora, A. M., & Ucan, O. N (2006). Separation of Magnetic Field Data Using Differential Markov Random Field (DMRF) Approach. *Geophysics*, (71): 125-134.

[2]. Geman, S., & Geman, D (1984). Stochastic Relaxation, Gibbs Distributions, and the Bayesian restoration of images. *IEEE PAMI*, (6): 721-741.

[3]. Derin, H., & Elliot, A.H (1987). Modelling ans segmentation of noisy and textured images using Gibbs Random Field. *IEEE PAMI*, (9): 39-55.

[4]. Dubes, R.C., & Jain, A (1989). Random field models in image analysis. *Journal of Applied Statistics*, (16): 131-162.

[5]. Uçan, O.N., Şen, B., Albora, A.M., & Özmen, A (2000). A New Gravity Anomaly Separation Approach: Differential Markov Random Field (DMRF). *Electronic Geosciences*, (5): 1-1.

[6]. Uçan, O.N. & Albora, A.M (2000). Markov Rastgele Alanlar Yöntemi Kullanılarak Elazığ-Gölalan krom sahasının incelenmesi. *App. Earth Sciences-Kocaeli University*, (1): 107-117.

[7]. Uçan O.N. & Albora, A. M (2001) Markov Rasgele Alanlar Yöntemi Kullanılarak HİTİT HUWASI kutsal sahasının görüntülenmesi. *Marmara Üniversitesi Dergisi*, (15): 35-38.

[8]. Albora, A. M., Uçan, O.N. & Üçer, A (2002). Markov Random Filtre Yöntemi Kullanılarak Sivas Divriği-Dumluca Maden Sahasının Rezervinin Belirlenmesi. *App. Earth Sciences-Kocaeli University*, (1): 113-124.

[9]. Albora, A. M., Ucan, O. N. & Aydoğan, A (2007). Modeling Potential Fields Sources in The Gelibolu Peninsula (Western Turkey) Using A Markov Random Field Approach. *Pure and Applied Geophysics*, (164): 1057-1080.

[10]. Uçan, O.N. & Albora, A. M (2009). Evaluation of Ruins of Hitite Empire in Sivas-Kusakli Region Using Markov Random Field (MRF). *Near Surface Geophysics*, (7):111-122.

[11]. Uçan, O.N. & Albora, A. M (2009). Evaluation of Ruins of Hitite Empire In Sivas-Kusakli Region Using Markov Random Field (MRF). *Near Surface Geophysics*, (7): 111-122.

[12]. Demir, D., Bilim F., Aydemir, A. & Ateş A (2012). Modelling of Thrace Basin, NW Turkey using gravity and magnetic anomalies with control of seismic and borehole data. *Journal of Petroleum Science and Engineering*, (86): 44–53.

[13]. Üşümezsoy, Ş (2005). Vatandaş için deprem rehberi Türkiye'de deprem riski ve Marmara depremi, İleri Yayınları, İstanbul.

[14]. Gökaşan, E., Gazioğlu, C., Alpar, B., Yücel, Z.Y., Ersoy, Ş., Gündoğdu, O., Yaltırak, C. & Tok, B (2002). Evidences of NW extension of the North Anatolian Fault Zone in the Marmara Sea; a new approach to the 17 August 1999 Marmara Sea earthquake. *Geo-Marine Lett.*, (21): 183-199.

[15]. Gökaşan, E., Ustaömer, T., Gazioğlu, C., Yücel, Z.Y., Öztürk, K., Tur, H., Ecevitoğlu, B. & Tok, B (2003). Morpho-tectonic evolution of the Marmara Sea inferred from multi-beam bathymetric and seismic data. *Geo-Marine Letters*, (23/1): 19-33.

[16]. Şengör, A.M.C., Tüysüz, O., İmren, C., Sakınç, M., Eyidoğan, H., Görür, N., Le Pichon, X. & Rangin, C (2005). The North Anatolian Fault: A New Look. *Annu. Rev. Earth Planet. Sci*., (33): 1-75.

[17]. Çağlak, F., Albora, A. M. and Uçan, O. N (2006). Determination of the Fault Zone by Using Genetic Celluar Neular Network in the Thrace and the Marmara Sea. *IEEE 14th Signal Processing and Communications Applications (SIU)*.

[18]. Albora, A. M (2013). A View of Tectonic Structure of Marmara Region (NW Turkey) using Steerable Filters. *American Geophysical Union (AGU)*.

[19]. Albora, A. M (2014) Using Steerable Filter Detection of Tectonic Lines of the Marmara Region. *IEEE 22th Signal Processing and Communications Applications (SIU)*, 417-420.